

Supporting Information

Engineering Monodispersed 2 nm Sb₂S₃ Particles Embedded in Porphyrin-Based MOF-Derived Mesoporous Carbon Network via the Adsorption Method to Construct High- Performance Sodium-Ion Battery Anode

Shuya Zhao¹, Hongna Jia¹, Yao Wang¹, Na Ju¹, Xinyue Zhang¹, Ying Guo¹, Yiming Wang¹, Haipeng Wang¹, Suyan Niu¹, Yan mingLu², Lin Zhu², Hong-bin Sun*¹

¹ Department of Chemistry, Northeastern University, Shenyang 110819, People's Republic of China. E-mail: sunhb@mail.neu.edu.cn

² Department of Physics, Northeastern University, Shenyang 110819, People's Republic of China

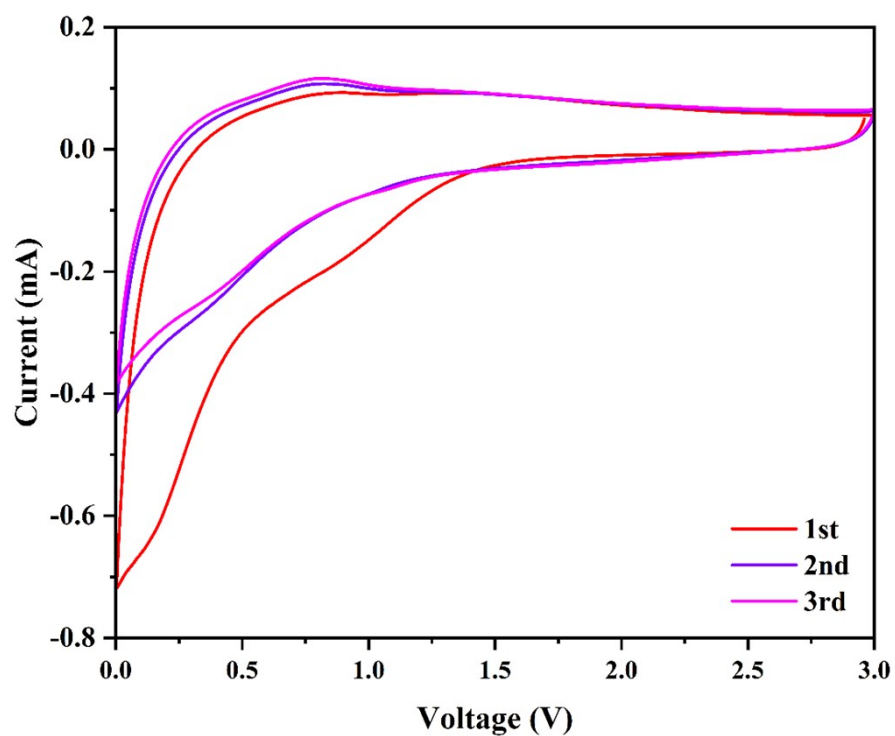


Figure S1 CV curves with a scan rate of $1.0 \text{ mV}\cdot\text{s}^{-1}$ of the CZM.

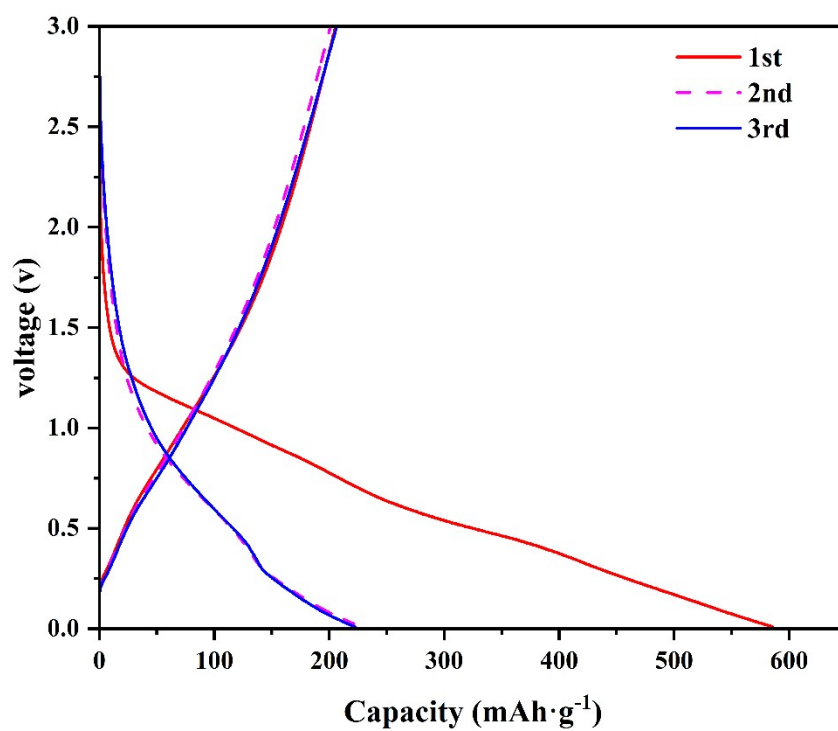


Figure S2 Galvanostatic charge-discharge curves at $0.1 \text{ A}\cdot\text{g}^{-1}$ of CZM.

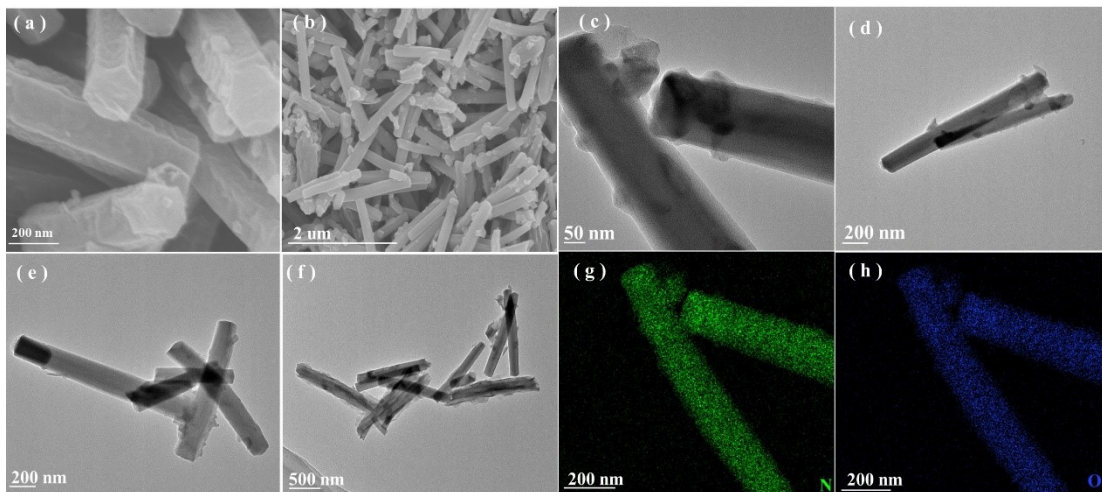


Figure S3 SEM images of PCN-222(a) and $\text{Sb}_2\text{S}_3/\text{CZM}$ (b). TEM (c, d, e, f) and images of $\text{Sb}_2\text{S}_3/\text{CZM}$. (g, h) EDS mapping analysis of $\text{Sb}_2\text{S}_3/\text{CZM}$.

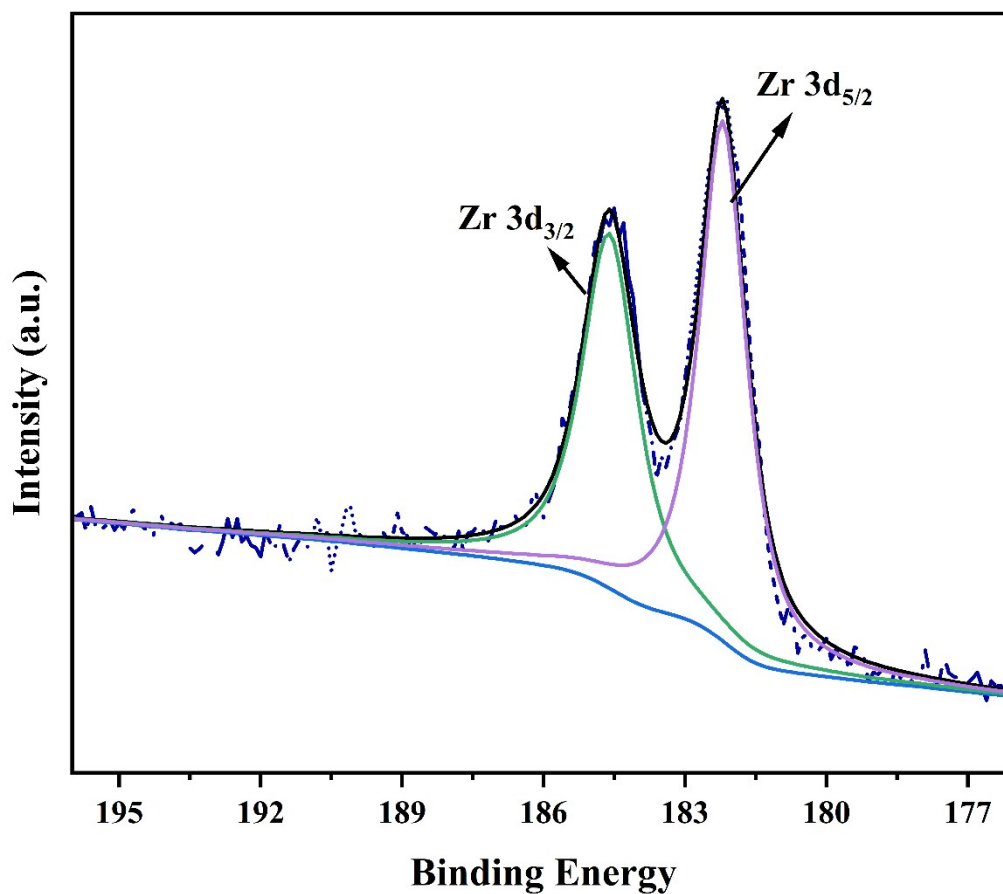


Figure S4 Zr 3d narrow scan spectra of $\text{Sb}_2\text{S}_3/\text{CZM}$.

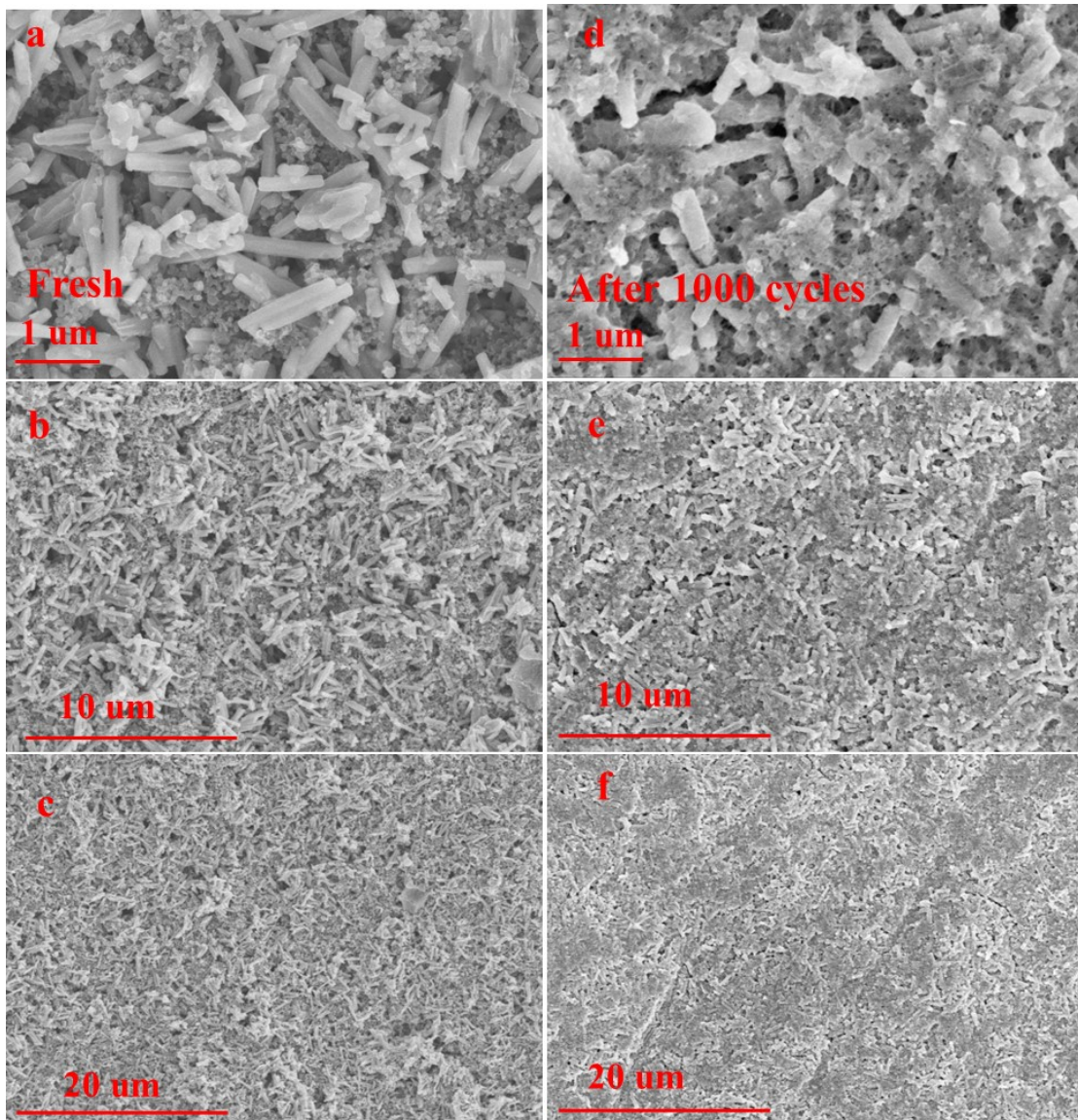


Figure S5 (a-c) SEM image of the original $\text{Sb}_2\text{S}_3/\text{CZM}$ electrode and (d-f) the $\text{Sb}_2\text{S}_3/\text{CZM}$ electrode after 1000 cycles.

Fig. S5 shows the micro-morphology of the original electrode sheet and the electrode sheet after 1000 cycles. It can be seen from the comparison of Fig. S5a and d that the morphology of the material after 1000 cycles has no obvious fracture or agglomeration. In addition, all of the columnar particles become not as smooth as the as prepared material, indicating the formation of SEI. From Fig. S5b, e, and Fig. S5c, f we can see that a dense SEI film is formed on the surface of the electrode after cycles. As can be seen from Fig. S5f, after a long cycle test, the surface of the electrode sheet basically keeps intact. This further reveals the reason why the $\text{Sb}_2\text{S}_3/\text{CZM}$ electrode has preminent cycling stability.



Figure S6 (a) Rate capability (b) cycling performance of $\text{Sb}_2\text{S}_3/\text{CZM}$ ($1.0\sim 1.2 \text{ mg cm}^{-2}$).

From Fig. S6a, we can see the $\text{Sb}_2\text{S}_3/\text{CZM}$ shows good rate capacity at various current rates from 1 A g^{-1} to 10 A g^{-1} . It delivered reversible capacities of 439, 405, 355, 319, 273, 235 $\text{mAh}\cdot\text{g}^{-1}$. When the current density returns to $1 \text{ A}\cdot\text{g}^{-1}$, the sample electrode recovers a specific capacity of $430 \text{ mAh}\cdot\text{g}^{-1}$. The results show good stability and reversibility again. At the same time, the cycling performance of $\text{Sb}_2\text{S}_3/\text{CZM}$ composite was investigated at the current density of 3 A g^{-1} for 500 cycles (Fig. S6b). The $\text{Sb}_2\text{S}_3/\text{CZM}$ composite proves a relative stable cycling performance, showing a reversible capacity of $310 \text{ mAh}\cdot\text{g}^{-1}$ at $3 \text{ A}\cdot\text{g}^{-1}$ after 500 cycles with a high capacity retention of 87.0%.

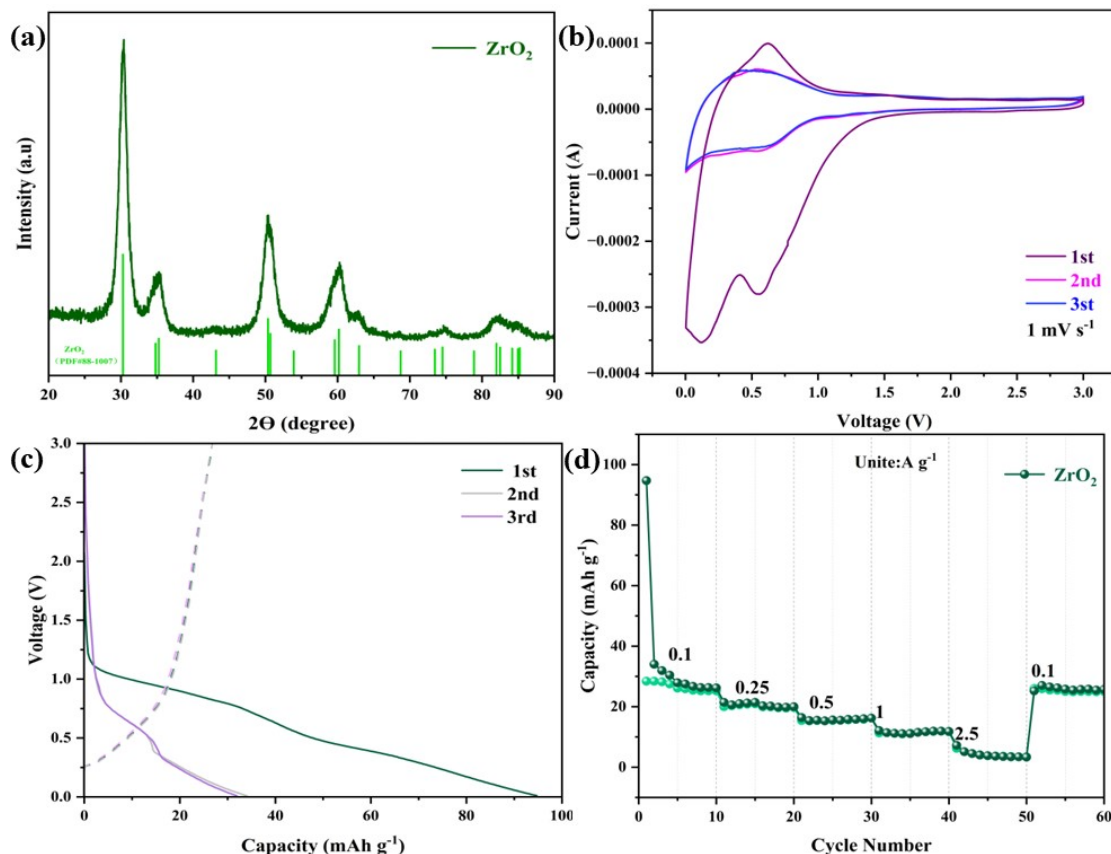


Figure S7 (a) XRD pattern of ZrO_2 . (b) CV curves with a scan rate of $1.0 \text{ mV} \cdot \text{s}^{-1}$ of the ZrO_2 . (c) Galvanostatic charge-discharge curves at $0.1 \text{ A} \cdot \text{g}^{-1}$ of ZrO_2 . (d) Rate performance of ZrO_2 .

Noticing the existence of ZrO_2 in $\text{Sb}_2\text{S}_3/\text{CZM}$, we tested the electrochemical performance of ZrO_2 for illustrating its contribution. We calcined CZM at 800°C in air to remove the carbon to obtain ZrO_2 . Fig.S7a illustrated the XRD pattern of ZrO_2 is consistent with zirconium oxide (JCPDS 88-1007), indicating the pure phase of ZrO_2 . Then we used the obtained ZrO_2 to assemble the coin cells following the same procedure of $\text{Sb}_2\text{S}_3/\text{CZM}$. Fig.S7b shows the initial three cycles cyclic voltammetry (CV) curves of ZrO_2 electrode at a scan rate of $1 \text{ mV} \cdot \text{s}^{-1}$, while the Charge-discharge profile is displayed in Fig.S7c and Fig.S7d shows the rate capacity test at various current rates from $0.1 \text{ A} \cdot \text{g}^{-1}$ to $2.5 \text{ A} \cdot \text{g}^{-1}$. It delivered very poor capacities, which is no more than the contribution of conductive carbon black added. This indicates that ZrO_2 has no Na ion storage capacity, and it contributes no electrochemical performance to the $\text{Sb}_2\text{S}_3/\text{CZM}$ composite.

Table S1 The impedance parameters of the Sb₂S₃/CZM and CZM electrode before cycling and after 700 cycles

Sample	Before cycling		After 700cycles	
	R _f (Ω)	R _{ct} (Ω)	R _f (Ω)	R _{ct} (Ω)
Sb ₂ S ₃ /CZM	--	998	10	178
CZM	--	650	15	220

Table S2 The rate capacity of Sb₂S₃/CZM electrode and CZM electrode.

Current density (A g ⁻¹)	0.1	0.25	0.5	1	2.5	3	5	7	10
Specific capacity (mAh g ⁻¹) of Sb ₂ S ₃ /CZM	550	526	508	449	413	378	330	302	266
Specific capacity (mAh g ⁻¹) of CZM	215	173	156	138	118	109	95	85	75

Table S3 The rate performance of Sb₂S₃/CZM electrode and CZM electrode.

	1 A g ⁻¹ Vs. 0.1 A g ⁻¹	10 A g ⁻¹ Vs. 1 A g ⁻¹
Capacity retention of Sb ₂ S ₃ /CZM	81.6%	59.2%
Capacity retention of CZM	64.2%	54.3%

Table S4 The electrochemical cycle stability and rate performance of Sb₂S₃/CZM electrode with other Sb₂S₃ based electrodes for SIBs from the recent published literature.

Ref	sample	Rate current density	Specific capacity	Cycle stability (Capacity retention)
This work	Sb ₂ S ₃ /CZM	0.1 A g ⁻¹ ~10 A g ⁻¹	550mAh g ⁻¹ (0.1 A g ⁻¹) 330mAh g ⁻¹ (5 A g ⁻¹) 266mAh g ⁻¹ (10 A g ⁻¹)	90.0% (1 A g ⁻¹ ,500 cycles) 88.9% (3 A g ⁻¹ ,1000 cycles)
35	Sb ₂ S ₃ -Nns	0.05 A g ⁻¹ ~5 A g ⁻¹	~500 mAh g ⁻¹ (0.05 A g ⁻¹) ~300 mAh g ⁻¹ (5 A g ⁻¹)	71.8% (1 A g ⁻¹ ,120 cycles)
38	Sb ₂ S ₃ /C	0.2 A g ⁻¹ ~6.4 A g ⁻¹	700mAh g ⁻¹ (0.1 A g ⁻¹) 180mAh g ⁻¹ (6.4 A g ⁻¹)	78.3% (0.2 A g ⁻¹ ,70 cycles)
39	Sb ₂ S ₃ /RGO	0.1 A g ⁻¹ ~1.5 A g ⁻¹	367 mAh g ⁻¹ (0.1 A g ⁻¹) 182 mAh g ⁻¹ (1.5 A g ⁻¹)	74.1% (0.1 A g ⁻¹ ,100 cycles)
37	MWNTs@ Sb ₂ S ₃ @PPy	0.05 A g ⁻¹ ~5 A g ⁻¹	560 mAh g ⁻¹ (0.1 A g ⁻¹) 280 mAh g ⁻¹ (5 A g ⁻¹)	83.8% (0.1 A g ⁻¹ , 85 cycles)
17	Sb ₂ S ₃ @N-C/RGO-2	0.1 A g ⁻¹ ~10 A g ⁻¹	455 mAh g ⁻¹ (0.1 A g ⁻¹) 201 mAh g ⁻¹ (10 A g ⁻¹)	70.0% (1 A g ⁻¹ ,1500 cycles)
36	Sb ₂ S ₃ @m-Ti ₃ C ₂ T _x	0.02 A g ⁻¹ ~1 A g ⁻¹	412 mAh g ⁻¹ (0.1 A g ⁻¹) 255 mAh g ⁻¹ (1 A g ⁻¹)	62.0% (0.1 A g ⁻¹ ,100 cycles)
34	SNCFs	0.05 A g ⁻¹ ~2 A g ⁻¹	417 mAh g ⁻¹ (0.1 A g ⁻¹) 244 mAh g ⁻¹ (2 A g ⁻¹)	66.0% (0.05 A g ⁻¹ ,50 cycles)
40	Sb ₂ S ₃ /SCS	0.1 A g ⁻¹ ~1 A g ⁻¹	636 mAh g ⁻¹ (0.1 A g ⁻¹) 263 mAh g ⁻¹ (1 A g ⁻¹)	70.8% (0.05 A g ⁻¹ ,100 cycles)
41	Sb ₂ S ₃ /S-CM	0.1 A g ⁻¹ ~2 A g ⁻¹	801 mAh g ⁻¹ (0.1 A g ⁻¹) 481 mAh g ⁻¹ (2 A g ⁻¹)	84.3% (0.1 A g ⁻¹ ,150 cycles)
42	Sb ₂ S ₃ /CNT	0.1 A g ⁻¹ ~3 A g ⁻¹	874 mAh g ⁻¹ (0.1 A g ⁻¹) 411 mAh g ⁻¹ (3 A g ⁻¹)	81.0% (0.1 A g ⁻¹ , 50 cycles)

Notes

The authors declare no competing financial interest.

Acknowledgements

We gratefully acknowledge the financial support from the National Natural Science Foundation of China (No. 21872020).